Research Note

On the Mechanism of Visible-Light Sensitized Photo*sulfoxidation* of Toluidine Blue O

Jennifer Otero-González,[1‡] Whitney Querini-Sanguillén,[1‡] Daniel Torres-Mendoza,[2,3,4] Ikhil Yevdayev,[5] Sharon Yunayev,[5] Kamrun Nahar,[5,6] Barney Yoo,[7] Alexander Greer,[5,6*] Denis Fuentealba,[8*] and José Robinson-Duggon[1,9*]

[1]*Departamento de Bioquímica, Facultad de Ciencias Naturales, Exactas y Tecnología, Universidad de Panamá, Panamá 0824, República de Panamá*

[2]*Laboratorio de Bioorgánica Tropical, Facultad de Ciencias Naturales, Exactas y Tecnología, Universidad de Panamá, Panamá 0824, República de Panamá.*

[3]*Departamento de Química Orgánica, Facultad de Ciencias Naturales, Exactas y Tecnología, Universidad de Panamá, Panamá 0824, República de Panamá.*

[4]*Vicerrectoría de Investigación y Postgrado, Universidad de Panamá, Panamá 0824, República de Panamá.*

[5] *Department of Chemistry, Brooklyn College, City University of New York, Brooklyn, New York 11210, United States.*

[6] *Ph.D. Program in Chemistry, The Graduate Center of the City University of New York, 365 Fifth Avenue, New York, New York 10016, United States.*

[7] *Department of Chemistry, Hunter College, City University of New York, New York 10065, United States.*

[8] *Laboratorio de Química Supramolecular y Fotobiología, Escuela de Química, Facultad de Química y de Farmacia, Pontificia Universidad Catolica de Chile, Vicuna Mackenna 4860, Macul, Santiago, Chile*

[9] *Sistema Nacional de Investigación (SNI), Secretaría Nacional de Ciencia, Tecnología e Innovación (SENACYT), Panamá, República de Panamá*

‡ Equal contribution of authors

*Corresponding author e-mail: agreer@brooklyn.cuny.edu (Alexander Greer), dlfuente@uc.cl (Denis Fuentealba), jose.robinson@up.ac.pa (José Robinson-Duggon)

TABLE OF CONTENTS GRAPHIC

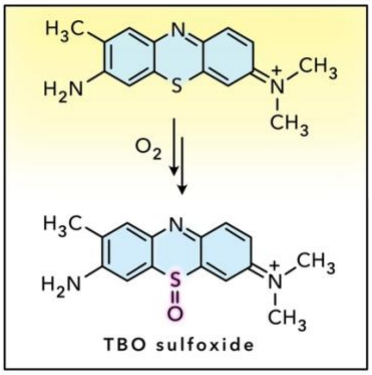

TOC SYNOPSIS: Experimental and theoretical strategies for deducing mechanistic paths of photobleaching are challenging. Progress has been made based with the self-sensitized photooxidation toluidine blue O (TBO), leading to TBO sulfoxide and other products. This is a unique albeit minor self-sensitized photooxidation path, where the TBO sulfoxide arises by a type I process. Density functional theory results point to either peroxyl radical or thiadioxirane intermediate to reach the TBO sulfoxide.

ABSTRACT

We report on the formation of toluidine blue O (TBO) sulfoxide by a self-sensitized photooxidation of TBO. Here, the photo*sulfoxidation* process was studied by mass spectrometry (MS) and discussed in the context of photodemethylation processes which both contribute to TBO

consumption over time. Analysis of solvent effects with D_2O, H_2O, and CH_3CN along with product yields and MS fragmentation patterns provided mechanistic insight to TBO sulfoxide's formation. The formation of TBO sulfoxide is minor and detectable up to 12% after irradiation of 3 h. The photosulfoxidation process is dependent on oxygen wherein instead of a type II (singlet oxygen, $^1O_2$) reaction, a type I reaction involving TBO to reach the TBO sulfoxide is consistent with the results. Density functional theory results point to the formation of the TBO sulfoxide by the oxidation of TBO via transiently formed peroxyl radical or thiadioxirane intermediates. We discover that the TBO photosulfoxidation arises competitively with TBO photodemethylation with the latter leading to formaldehyde formation.

INTRODUCTION

Self-sensitized photooxidation reactions play a significant role in a variety of fields, including organic synthesis and pollutant degradation (1,2). For this reason, several studies have endeavored to better understand the mechanisms of self-sensitized photooxidation reactions in type I and type II reactions (Figure 1A). Medical and other organic pollutants with intrinsically self-sensitizing structures, often undergo type II photooxidation reactions. In 2021, a combined DFT and experimental study (3), an application of the self-sensitized type I photooxidation of toluidine blue O (TBO) was demonstrated. In that work, a synthetically significant demethylation was shown to occur (Figure 1B).

While candidate photooxidation paths could be type I (oxygen radicals) or type II ($^1O_2$) (4-6), for TBO the evidence pointed to the former. Here, methyl groups were shown to depart as formaldehyde molecules. This single carbon atom loss process can be contrasted to two carbon

loss processes. For example, the self-sensitized photooxidation of heptamethine cyanine (7) and rhodamine B (8) leads to the loss of ethene and ethyl groups, respectively. Loss processes are not limited to carbon fragments, however. Sensitizers that bear sulfur groups can involve both sulfur atom loss and oxidation processes. For example, a dimeric BODIPY sulfoxide was reported to undergo an SO extrusion process (9). Figure 1C shows an example of a sulfur-substitued BODIPY derivative that cycles reversibly as a redox sensor between the sulfide and sulfoxide forms (10).

How TBO self-sensitized photooxidation leads to not only demethylation, but also sulfoxidation paths, remains to be clarified. In the present work, we consider TBO in the self-sensitized photooxidative formation of TBO sulfoxide. In the present work, evidence points to the sulfoxidation of TBO's sulfur by a type I reaction, with no evidence to support a type II reaction. By comparison, organic sulfides such as diethyl sulfide and thietane undergo type II reactions that form sulfoxide through a persulfoxide intermediate, $R_2S^+OO^-$ (11-15). TBO's sulfur site appears similar to diaryl and diphenyl sulfide sites, which are usually unreactive with $^1O_2$. Indeed, other reports have appeared on type I photooxidations of dibutyl sulfide and dibenzothiophene (16-19), as well as *N*-methyl phenothiazine in a type I reaction in homogeneous media and a type II reaction in micellar media (20,21). Self-sensitized reactions of metal thiolanes (22-25) and thiochroman-fused C_{60} (26) have lead to type II reactions, where $^1O_2$ can react at the sulfide sites to produce sulfoxides and sulfones. As we will see, experimental and theoretical evidence suggests that the sulfoxidation of TBO occurs through a type I self-sensitized reaction.

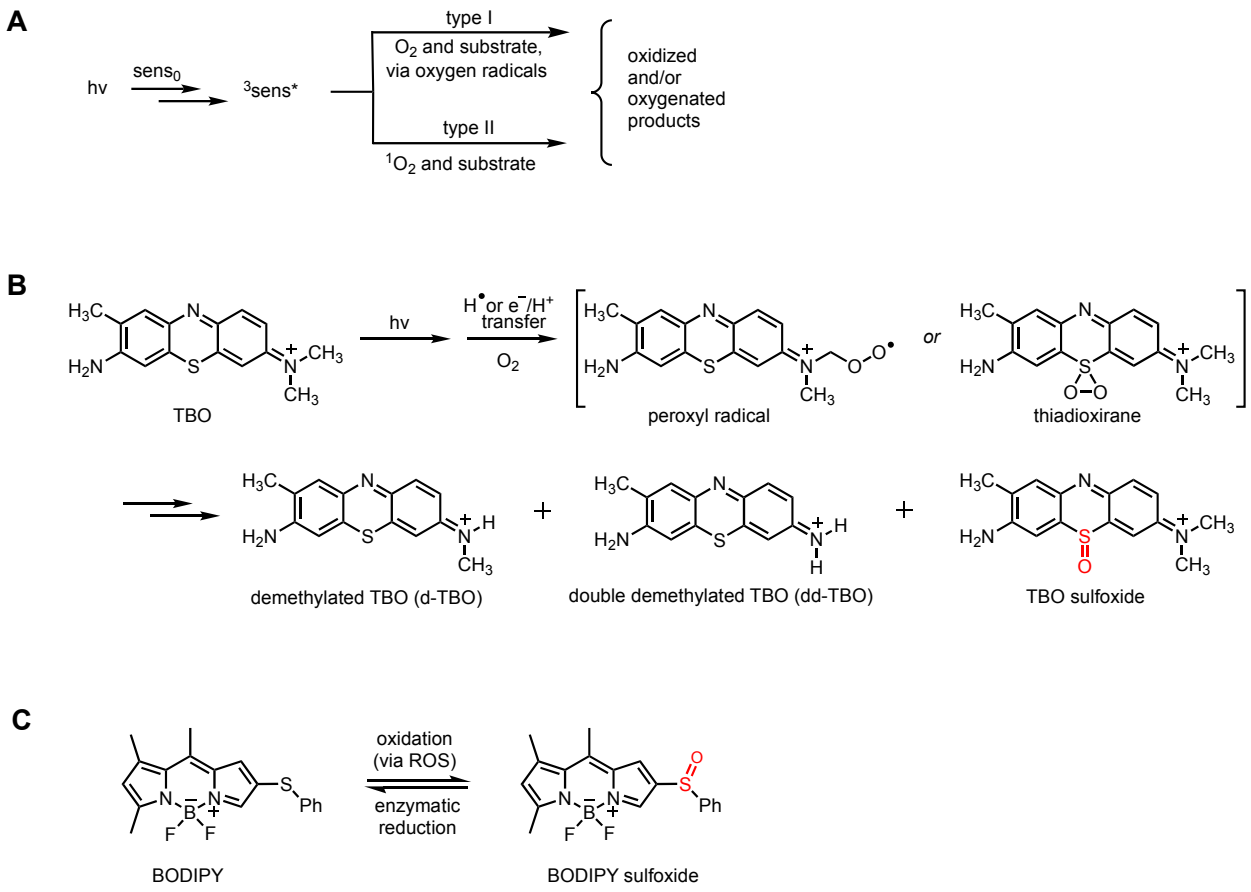

Figure 1. (A) An illustration of type I and type II photosensitized oxidation processes. (B) Self-sensitized type I TBO demethylation path described previously (see ref. 3) and formation of the TBO sulfoxide as a by-product, which is the subject of the current work. Candidate intermediates to reach the TBO sulfoxide include a peroxyl radical or thiadioxirane. (C) Literature example of a BODIPY redox sensor that cycles between the corresponding sulfide with reactive oxygen species and the sulfoxide in a reversible enzymatic process (see ref. 10), bearing rough similarity to the formation of TBO sulfoxide.

RESULTS AND DISCUSSION

We report here an mass spectrometry (MS) study of the photo*sulfoxidation* reaction of TBO in three solvents (CH_3CN, H_2O and D_2O). Firstly, purification of TBO is needed as the commercial TBO sample contains significant levels of impurities, especially when stored over time in room light. The concentration of TBO used was ~12.5 μM in all solvents (absorbance of ~0.5) as it can be seen in Figure 2. TBO was irradiated in air-saturated solutions for 1-3 h and MS spectra where TBO sulfoxide appears as a small peak at *m/z* 286.1. Due to the resolution of the MS, TBO sulfoxide sometimes also appears as *m/z* 286.2. Upon irradiation in CH_3CN, TBO sulfoxide increases from 9.8±1.2% at 1 h to 12.2±1.5% after 3 h (Table 1), whereas in H_2O, it increases to 7.3±0.9% at 1 h, but decreases to 4.0±0.5% after 3 h. This suggests that at longer irradiation times in H_2O lead to some TBO sulfoxide decomposition (Table 1).

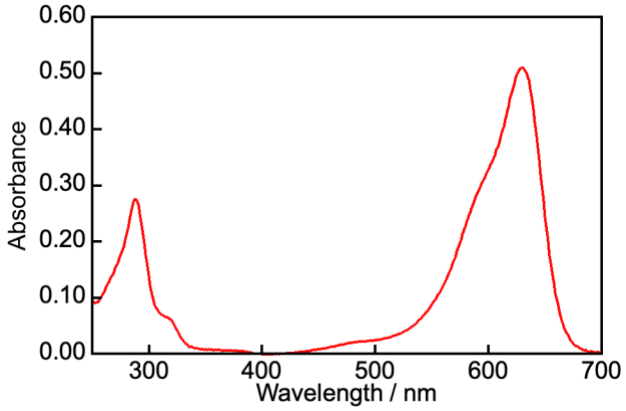

Figure 2. UV-visible spectra of TBO in CH_3CN.

The observed MS/MS fragmentation pattern is consistent with the TBO sulfoxide at *m/z* 286.1 (Figure 3c). The mass spectra of the TBO samples were recorded in the 3 solvents with irradiation times of 1-3 h (Figures S1-S14, Supporting Information). The photoformation of TBO

sulfoxide was found to depend on the presence of oxygen. Sparging of the solution with air (21% O_2) led to an increased TBO sulfoxide signal by 29% compared to an N_2-sparged acetonitrile solution. Indeed, under N_2 atmosphere, no increase in the TBO sulfoxide signal was observed. Thus, while TBO sulfoxide is a minor product that can conceivably arise by either a type I or type II oxidation mechanism. We have reported previously that TBO undergoes mainly a type I photosensitized degradation (3), in which TBO also produces $^1O_2$ with a quantum yield (Φ_Δ) of 0.14-0.18 (27,28). Thus, we examined the reaction to probe whether TBO sulfoxide arises by the self-sensitized formation $^1O_2$. When CH_3CN was exchanged for H_2O, the $^1O_2$ lifetime (τ_Δ) decreases from 55 μs (29) to 3.5 μs (30), and the amount of TBO sulfoxide formed would be expected to decrease significantly. However, TBO sulfoxide yield only varied by ~3-fold after 3 h of irradiation. Moreover, in D_2O the TBO sulfoxide yield did not increase significantly compared to H_2O; the yield was 4.6±0.6% in D_2O and 4.0±0.5% in H_2O after 3 h of irradiation. This result is inconsistent with a type II mechanism. Because the τ_Δ in D_2O is some 19-fold greater than in H_2O, if the type II mechanism was operative, TBO sulfoxidation would have been greater yielding in D_2O than H_2O (31). TBO sulfoxide is one of several compounds formed in the reaction.

In the reaction, TBO sulfoxide is formed in minor amounts, and itself decomposes over time, particularly in H_2O after 2 h of irradiation. In addition to the TBO sulfoxide formed, TBO photodegradation ocurrs through the loss of the methyl groups from the dimethylammonium ion moiety (Figure 3b). In the dark, the MS signal for TBO is prominent at *m/z* 270.1 (Figure 3a), whereas after 2 h of irradiation mono-demethylated TBO (d-TBO) appears at *m/z* 256.0 and is the main product (Figure S4, Supporting Information). After 3 h irradiation, double-demethylated TBO (dd-TBO) appears at *m/z* 242.0 and becomes the main product (Figure 3b). These MS data are consistent with previous results on the formation of d-TBO and dd-TBO (3). The current

observed MS/MS fragmentation patterns obtained are consistent with TBO at *m/z* 270.1, d-TBO at *m/z* 255.9, and dd-TBO at *m/z* 242.1. Not detected was the photosulfoxidation of the d-TBO and dd-TBO to reach d-TBO sulfoxide at *m/z* 272 and dd-TBO sulfoxide at *m/z* 258, respectively.

Table 1 shows MS data that the self-photooxidation of TBO led to TBO sulfoxide in about 0.6% greater amounts in D_2O than H_2O (cf. 4.6% to 4.0%). Table 2 shows GCMS relative abundance data that were collected for quenching studies carried out with the $^1O_2$ quencher sodium azide (2 mM) in CH_3CN leading to only a modest reduction in the production of TBO sulfoxide (cf. 10% to 9%). A more substantial 4% reduction in the TBO sulfoxide relative abundance (cf. 10% to 6%) was observed when the photoreaction carried out in the presence of the radical scavenger D-mannitol (15 mM). In the presence of D-mannitol, the relative abundance of d-TBO also declined (cf. 72% to 12%), and the relative abundance of dd-TBO declined as well from 18% to 5%. Thus, the relative abundance of TBO sulfoxide, d-TBO, and dd-TBO were less effected by the presence of the $^1O_2$ quencher sodium azide and more effected by the presence of the radical scavenger D-mannitol. Experiments were also carried out to assess whether superoxide radical anion was formed in the TBO photoreaction. Figure S15 (Supporting Information) shows that the appearance of a prominent absorption band for reduced cytochrome C at 550 nm did not materialize. That no changes were observed in the presence or absence of superoxide dismutase (SOD) points to a lack of evidence for superoxide radical anion under our experimental conditions (32,33).

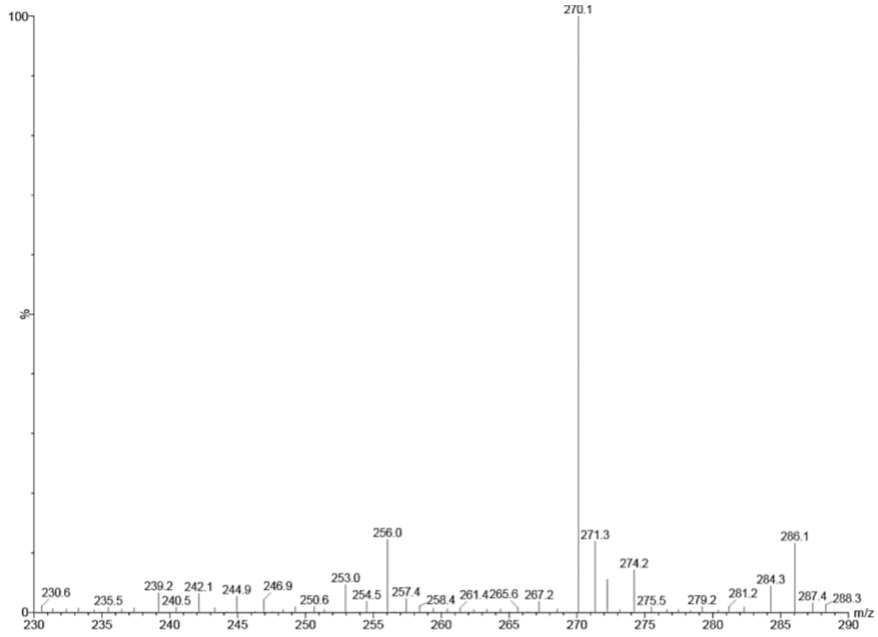
100
%
0
270.1
256.0
271.3
286.1
274.2
253.0
284.3
230.6
239.2
242.1
244.9
246.9
235.5
240.5
250.6
254.5
257.4
258.4
261.4
265.6
267.2
275.5
279.2
281.2
287.4
288.3
230
235
240
245
250
255
260
265
270
275
280
285
290
m/z

(a)

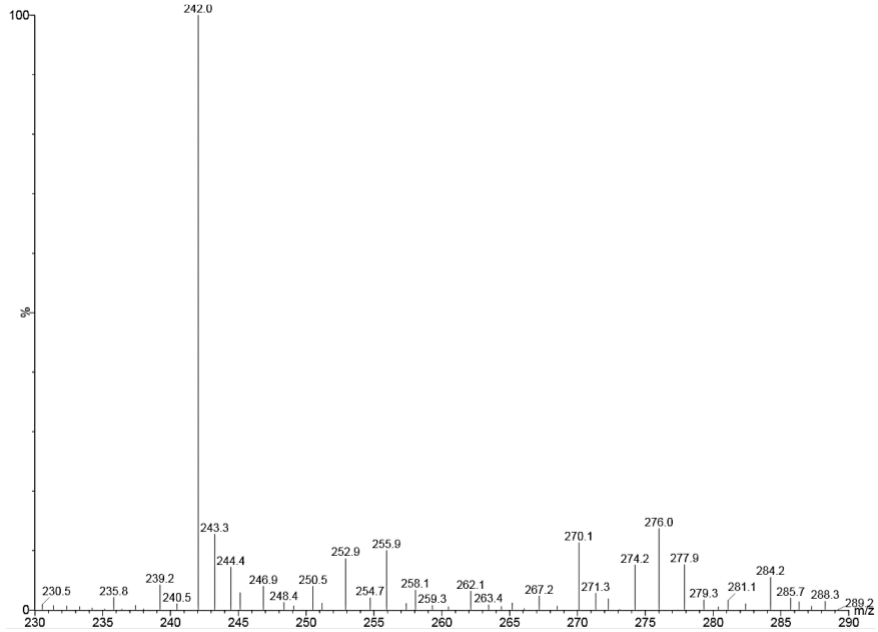
100
%
0
242.0
243.3
276.0
270.1
252.9
255.9
244.4
274.2
277.9
284.2
239.2
246.9
250.5
230.5
235.8
240.5
248.4
254.7
258.1
259.3
262.1
263.4
267.2
271.3
279.3
281.1
285.7
288.3
289.2
230
235
240
245
250
255
260
265
270
275
280
285
290
m/z

(b)

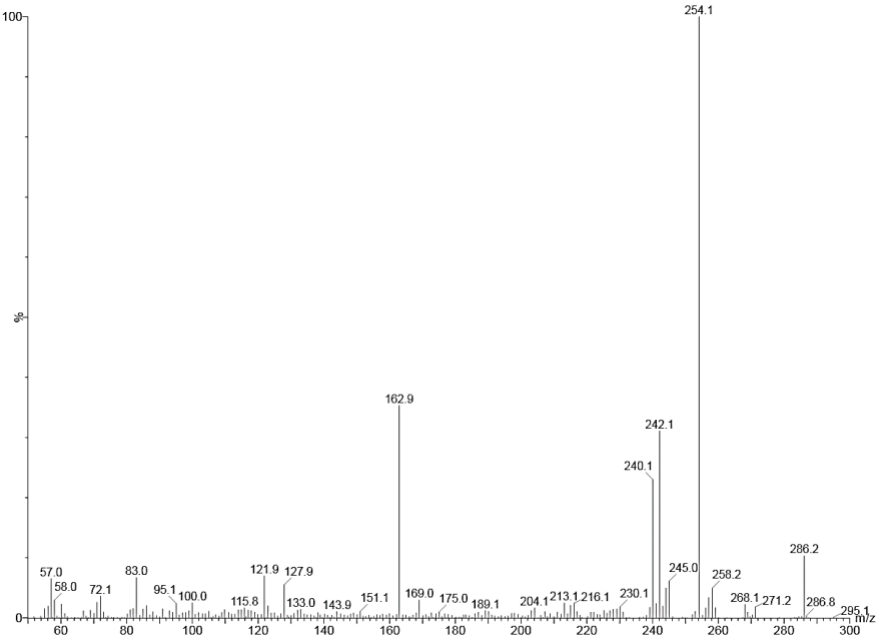

(c)

Figure 3. MS spectra of TBO sample in CH_3CN: (a) in the dark containing mainly TBO (*m/z* 270.1) and trace TBO sulfoxide (*m/z* 286.1), (b) after irradiation for 3 h showing an increase in TBO sulfoxide relative to TBO, in the presence of mono-demethylated TBO (d-TBO, *m/z* 255.9) and double-demethylated TBO (dd-TBO, *m/z* 242.0), and (c) MS/MS spectrum of TBO sulfoxide after 3 h irradiation for further evidence that the *m/z* 286.2 is the sulfoxide and comes from TBO sulfoxide.

Table 1. LCMS detection of the visible-light degradation of TBO in different solvents yielding dd-TBO, d-TBO, and TBO sulfoxide [a]

Solvent	Ion	*m/z* [b]	1 h	2 h	3 h
			Relative abundance		
CH_3CN	TBO	270.1	100.0	67.5	11.3
	TBO sulfoxide	286.1	9.8 (9.8%) [c]	6.3 (9.4%) [c]	1.4 (12.2%) [c]
	d-TBO	256.0	72.0	100.0	10.0
	dd-TBO	242.1	18.3	45.1	100.0
H_2O	TBO	270.1	100.0	100.0	100.0
	TBO sulfoxide	286.2	7.3 (7.3%) [c]	6.6 (6.6%) [c]	4.0 (4.0%) [c]
	d-TBO	256.1	9.1	9.3	9.9
	dd-TBO	242.2	1.0	0.2	0.1
D_2O	TBO	270.1			68.2
	TBO sulfoxide	286.2			3.2 (4.6%) [c]
	d-TBO	256.1			64.1
	dd-TBO	242.2			12.0

[a] Abbreviations: mono-demethylated TBO is d-TBO, and double-demethylated TBO is dd-TBO. [b] The *m/z* values have errors of ±0.2 amu; for example, the d-TBO can appear at 255.9, 256.0, and 256.1 amu in the spectra. [c] The % yield of TBO sulfoxide is shown in parentheses and is calculated from its relative abundance with respect to TBO. The reaction was carried out at room temperature (26 °C) where 12.5 µM TBO was irradiated for 1 h, 2 h and 3 h with a white light-emitting diode (LED) lamp, temperature color

6500 K and 2100 Lumens (Lm). Samples were irradiated with an illuminance of approximately 32,400 lux in the presence of oxygen. Samples were not sparged with air or O_2 during the course of the photoreaction. Solvents were CH_3CN LCMS hypergrade, H_2O LCMS grade, and D_2O NMR-grade.

Table 2. GCMS detection of the visible-light degradation of TBO in in CH_3CN yielding TBO sulfoxide, d-TBO, and dd-TBO [a]

Solvent	Ion	*m/z* [b]	Relative abundance [c]		
			no additive	azide ion	D-mannitol
CH_3CN	TBO	269−271	100	100	100
	TBO sulfoxide	285−287	10	9	6
	d-TBO	255−257	72	70	12
	dd-TBO	241−243	18	16	5

[a] Abbreviations: mono-demethylated TBO is d-TBO, and double-demethylated TBO is dd-TBO. [b] Ion extracted mass ranges (*m/z*) were analyzed for each compound. [c] The relative ion abundances are provided with respect to TBO. Reaction was carried out at room temperature where 2 mM TBO was irradiated for 1 h with ($400 < \lambda < 700$ nm) light. Samples were not sparged with air or O_2 over the course of the photoreaction.

MECHANISM AND SUMMARY

The proposed mechanism for a self-sensitized photosulfoxidation of TBO is shown in Figure 4. Path A shows that ^{3}TBO* sensitizes the formation of $^1O_2$, which converts back to ground-

state $^3O_2$ without TBO sulfoxide formation. TBO sulfoxide formation can arise by a type I (oxygen radicals) process involving a C-centered radical and formation of a peroxy radical (ROO·) followed by reaction with TBO to give the TBO sulfoxide (Path B) or alternatively by formation of thiadioxirane by electron transfer photooxidation (18,19) with a subsequent reaction with TBO to give the TBO sulfoxide (Path C). ROO· radicals display high electrophilicity in which their O-atom transfer is consistent with TBO's nucleophilic sulfide "S" site. As an aside, the ROO· can also dimerize and proceed by a Russell reaction or homolyze to reach an alkoxy radical (RO·), which demethylates to d-TBO and eventually dd-TBO (Path D). The native TBO can conceivably change its philicity from trapping of electrophilic oxidants (at the sulfide "S" site) to trapping of nucleophilic oxidants (at the sulfoxide "SO" site) similar to that reported for thianthrene 5-oxide (34). In our case, the conversion of TBO sulfoxide to TBO sulfone was not detected. While the experimental results point to a type I mechanism, we sought theoretical insight on the process leading to the TBO sulfoxide. In Figure 4, density functional theoretical (DFT) optimized structures show flat thiazines for TBO, C-centered radical, peroxy radical, and alkoxy radical, and curved thiazines for the thiadioxirane and TBO sulfoxide. The reaction of C-centered radical with triplet ground-state oxygen can readily form the peroxy radical, although its predicted exothermicity for O-atom to TBO is less than the thiadioxirane, which itself may arise from a type I process with TBO.

The data are consistent with a type I process and inconsistent with a type II process. The TBO demethylation process is oxygen dependent, forming the ROO· and then RO· with formaldehyde departure (Path D) (3), and is reminiscent of other reports of amine demethylations via photooxidation (35). As mentioned above, TBO produces $^1O_2$, which is similar to sensitizers,

252 such as pterins that produce $^1O_2$ as well as ROO·, RO·, HO·, and $O_2^{\bullet-}$ (36,37). Again, the data point
253 to a self-sensitized conversion of TBO to TBO sulfoxide by type I and not by $^1O_2$ (type II).

254 If a type II ($^1O_2$) mechanism were operating, solvent proticity would be expected to lead to
255 much greater TBO sulfoxide yields. For example, for diethyl sulfide (Et_2S) in CH_3OH, the
256 chemical quenching to the corresponding sulfoxide, Et_2SO, is ~100%, whereas in C_6H_6 it is only
257 5% (38-40). In CH_3OH, inhibition of physical quenching (conversion of $^1O_2$ to ground-state $^3O_2$)
258 is thought to initially form $R_2S^+OO^-$, and then convert to H-bonded or solvent stabilized sulfurane
259 (41). Indeed, sulfides with intramolecular OH groups yield products corresponding to transfer of
260 the alcohol oxygen to the sulfur (42).

261 It is known that aryl sulfides and dibenzothiophenes react very slowly if at all with $^1O_2$.
262 Indeed, Ph_2S has been used as a trapping agent for intermediates produced in sulfide/$^1O_2$ reaction
263 to react with hydroperoxysulfonium ylides (electrophilic oxidants) yielding Ph_2SO (43,44). Other
264 reports also point to type I photooxidation of dibenzothiophene (DBT) and 4,6-
265 dimethyldibenzothiophene (DMDBT) sensitized by *N*-methylquinolinium tetrafluoborate in
266 CH_3CN (18,19). DBT was selected as it contains no α-CH groups that could lead to *S*-
267 hydroperoxysulfonium ylide, an intermediate often found in reactions of sulfides with $^1O_2$ (19). In
268 refs. 18 and 19, evidence showed that the formation of DBT sulfoxide and DMDBT sulfoxide is
269 from the reaction between the $O_2^{\bullet-}$ and the $R_2S^{\bullet+}$. The results in ref. 18 also showed that the
270 sulfoxide formation was suppressed in the presence of benzoquinone, further bolstering the
271 assignment of a type I mechanism (18).

272 We find a solvent dependence in the percent yield of the TBO sulfoxide, which we attribute
273 to TBO aggregation. The TBO sulfoxide is higher yielding in CH_3CN (τ_Δ = 55 μs) at 12.2% yield,
274 compared to D_2O (τ_Δ = 65 μs) at 4.6% or H_2O (τ_Δ = 3.5 μs) at 4.0%. Because CH_3CN facilitates

275 higher yields, we surmise that some aggregation of TBO arises in D_2O and H_2O. Indeed, in H_2O
276 when TBO concentrations were raised from 2.0 μM to 12.5 μM, there was evidence for
277 aggregation. Whereas, in CH_3CN a TBO concentration of 12.5 μM appeared to be fully solvated,
278 although experiments required elevated TBO concentrations of 2 mM for GCMS detection of TBO
279 sulfoxide, d-TBO, and dd-TBO (Table 2). Somewhat similarly, a report of a phenothiazine-boron
280 dipyrromethene (BODIPY) dyad showed reduced aggregation and increased water solubility upon
281 *N*-conjugation to a tri(ethylene glycol) chain [$CH_3(OCH_2CH_2)_3$–] (45).
282

283

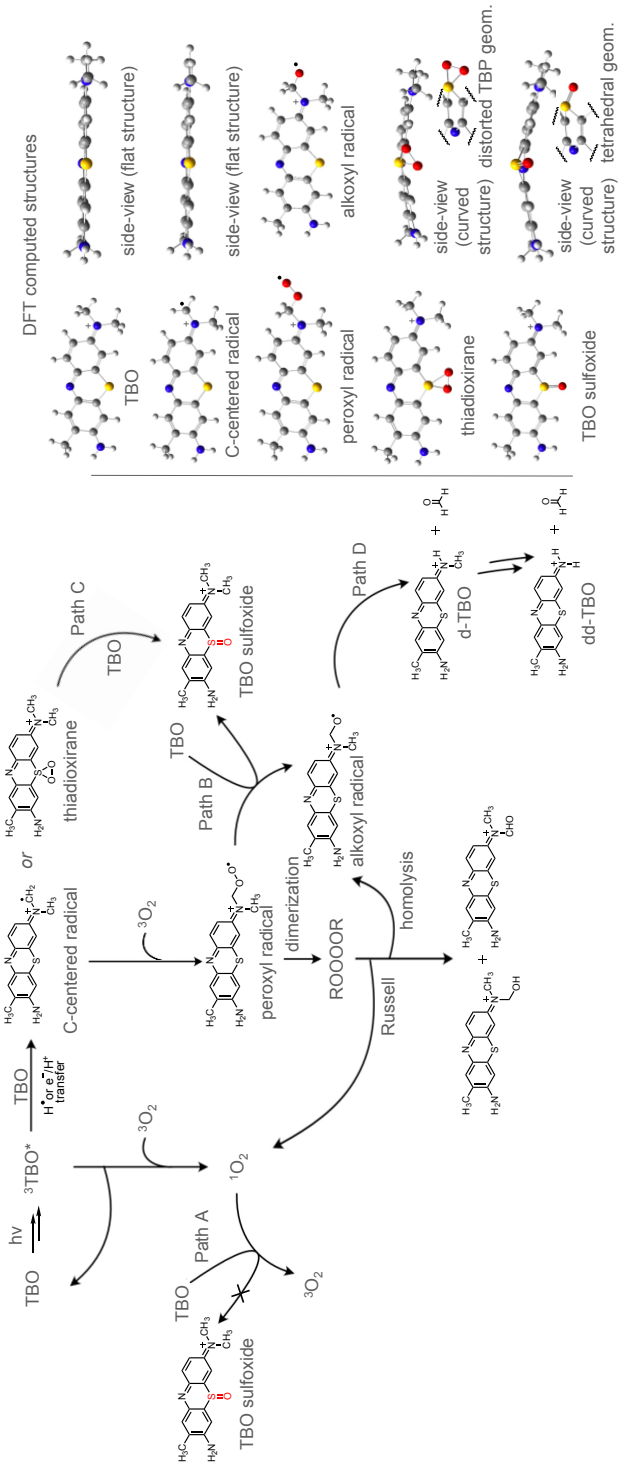

284

285 **Figure 4.** Proposed mechanism for the formation of TBO sulfoxide, d-TBO, dd-TBO and other

286 species by the self-sensitized photooxidation of TBO. The formation of the TBO sulfoxide can

arise by the oxidation of TBO with candidate peroxyl radical or thiadioxirane intermediates. The formation of products is dominated by oxygen radicals and radical ions (type I process) instead of by $^1O_2$ (type II process). The DFT calculations were carried out with M06-2X/6-31+G(d,p).

As was mentioned in the Introduction, a dimeric BODIPY sulfoxide was reported to undergo SO extrusion (9). However, in our case with TBO sulfoxide, inspection of decomposition products did not suggest an SO extrusion reaction. Furthermore, subsequent decomposition reactions of d-TBO and dd-TBO, or formation of TBO sulfone were not readily detected.

In conclusion, organic sulfides such as Et_2S chemically react with $^1O_2$ (11-15), but TBO and other aromatic sulfides like Ar_2S and DBT are chemically unreactive with $^1O_2$. As is evidenced here, TBO undergoes photo*sulfoxidation* by oxygen radicals in a proposed type I self-sensitized reaction. Future work could examine whether the conversion of TBO to TBO sulfoxide leads to a "turn on" fluorescence similar to a reaction of phenothiazine/BODIPY with ClO^- in reaching a phenothiazine sulfoxide/BODIPY (46). Fluorescence increases have also been observed in the conversion of dibenzothiophenes to dibenzothiophene sulfones (47).

METHODS

Chemicals. Toluidine blue O (TBO) was obtained from Sigma and purified to ≥95% using flash chromatography on silica gel with CH_3CH_2OH:HCl (99:1 v/v) as eluent. Sodium azide and D-mannitol were also purchased and used received from Sigma. Cytochrome C from equine heart (>95% purity) and superoxide dismutase from bovine erythrocytes (4743 U/mg) were obtained

and used as received from Sigma. Solvents CH_3CN, D_2O, H_2O, and CH_3CH_2OH, as well as HCl were used as received from Sigma-Aldrich. For column chromatography, 230-400 mesh silica gel was used. Stock solution of TBO in CH_3CN was prepared and aliquots were diluted to an absorbance of 0.5 at 626 nm for the irradiation experiments.

UV-visible spectrocopy and irradiation measurements. UV-visible spectra were collected in a Cary 60 UV/Vis using 1 cm pathlength cuvette. Samples were subjected to irradiation in a 1 cm pathlength cuvette for 1 h, 2 h, and 3 h in a custom-made irradiation chamber containing a 150 mm × 27.2 mm × 150 mm 30 W white light-emitting diode (LED) lamp, temperature color 6500 K and 2100 Lumens (Lm). Samples were irradiated with an illuminance of approximately 32369 lux measure with a HOBO data logger. Samples were not sparged with air or O_2 during the course of the photoreaction.

Mass spectrometry experiments. Two types of mass spectrometers were used. (1) UPLC-MS/MS spectrometry data were collected on a Waters XEVO® TQD spectrometer (Waters Corporation, Milford, MA, USA) supplied with an electrospray ionization (ESI) source. The samples were dissolved in CH_3CN (LCMS grade) and measured in positive ESI mode. The samples were filtered in a 0.22 μm filters and analyzed with the following conditions: probe temp 150 °C, cone voltage of 30 V, corona capillary voltage of 3.70 kV, desolvation temp 450 °C, desolvation gas flow 400 L/h, cone gas flow 30 L/h, infusion flow of 5.0 mL/min. Detection was performed in full scan mode in the range from 50−1500 *m/z*. The percent yield of TBO sulfoxide was assessed early in the photolysis (<2 h irradiation) relative to the parent TBO. After 2 h irradiation, d-TBO is the main product, and after 3 h irradiation dd-TBO is the main product. (2) GCMS spectrometry data was collected on a Varian Saturn 2000 GCMS (Varian Inc., Walnut Creek, CA, USA). The column used was a Supelco Analytical SP-233 fumed silica capillary (30

m × 0.25 mm × 0.2 um film thickness, catalog #24019). Here, the samples were dissolved in CH_3CN and measured in the electron impact (EI) mode. The TBO concentration was 2 mM, and for the additives was 2 mM azide ion and 17 mM D-mannitol. The settings included an injection temperature of 250 °C, a Helium flow of 1.2 mL/min, and a mass range from 35 to 650 *m/z*. An ion extract mode was used in the range of 269−271 *m/z* for TBO, 285−287 *m/z* for TBO sulfoxide, 255−257 *m/z* for d-TBO, and 241−243 *m/z* for dd-TBO. The yields of TBO sulfoxide, d-TBO, and dd-TBO were determined after photolysis (1 h irradiation) relative to the parent TBO. For these samples, irradiation was carried out with two 400-W metal halide lamps through a longpass ≥ 400-nm filter solution (1-cm 75 w/v% $NaNO_2$) at 26 °C.

Superoxide radical anion detection. Solutions containing cytochrome C (120 μM) and TBO (aprox. 12 μM) in water in the presence or absence of 250 U mL^{-1} of SOD were irradiated for 30 min with a 630 nm LED. Absorption spectra for the samples were measured every 5 min.

Theoretical section. We conducted DFT calculations using Gaussian-16 (48), in which compounds were optimized with M06-2X/6-31G(d,p) in the gas phase in a similar manner as reported recently (49). Unrestricted M06-2X/6-31G(d,p) calculations where conducted for the peroxyl radical and $^3O_2$, where the latter value incorporated the experimentally known singlet-triplet energy value of 22.5 kcal/mol, which was added to this calculated value of $^3O_2$. Harmonic vibrational frequency calculations were also carried out on the stationary points on the potential energy surface (PES).

Acknowledgments. J.O.-G., W.Q-S., and J.R.-D. thank Vicerrectoría de Investigación y Postgrado of Universidad de Panamá CUFI-2021-P-CNET-018, Sistema Nacional de Investigación (SNI) of SENACYT and Secretaría Nacional de Ciencia, Tecnología e Innovación

(SENACYT) of Panamá grant PFID-FID-2021-189 for financial support. D.T-M. thank Vicerrectoría de Investigación y Postgrado of Universidad de Panamá. D.F. thank FONDECYT Regular 1210583. I.Y, S.Y., K.M., and A.G. thank the National Science Foundation (CHE-2154133) for funding. This work used Expanse in the Extreme Science and Engineering Discovery Environment (XSEDE) cluster at the San Diego Supercomputer Center, which is supported by the NSF (ACI-1548562) through allocation CHE-210052. We thank Leda Lee for the graphic arts work.

SUPPORTINGINFORMATION

Additional supporting information may be found online in the Supporting Information section at the end of the article:

Figure S1. MS/MS spectrum of TBO sulfoxide in CH_3CN in the dark.

Figure S2. Mass spectrum of the TBO sample in CH_3CN after 1 h of irradiation.

Figure S3. MS/MS spectrum of TBO sulfoxide in CH_3CN after 1 h of irradiation.

Figure S4. Mass spectrum of the TBO sample in CH_3CN after 2 h of irradiation.

Figure S5. MS/MS spectrum of TBO sulfoxide in CH_3CN after 2 h of irradiation.

Figure S6. Mass spectrum of TBO in H_2O in the dark.

Figure S7. MS/MS spectrum of TBO sulfoxide in H_2O in the dark.

Figure S8. Mass spectrum of the TBO sample in H_2O after 1 h of irradiation.

Figure S9. MS/MS spectrum of TBO sulfoxide in H_2O after 1 h of irradiation.

Figure S10. Mass spectrum of the TBO sample in H_2O after 2 h of irradiation.

Figure S11. MS/MS spectrum of TBO sulfoxide in H_2O after 2 h of irradiation.

Figure S12. Mass spectrum of the TBO sample in H_2O after 3 h of irradiation.

Figure S13. MS/MS spectrum of TBO sulfoxide in H_2O after 3 h of irradiation.

Figure S14. Mass spectrum of the TBO sample in D_2O buffer after 3 h of irradiation.

Figure S15. Assessing whether superoxide radical anion is formed in the photoreaction. M062X/6-31G(d,p) computed structures and energetics.

REFERENCES

1. Ghogare, A. A. and A. Greer (2016) Using singlet oxygen to synthesize natural products and drugs. *Chem. Rev.* **116**, 9994-10034.
2. Xie, X., Z. Zhang, Y. Hu, H. Cheng (2018) A mechanistic kinetic model for singlet oxygen Mediated self-sensitized photo-oxidation of organic pollutants in water. *Chem. Eng. J.* **334**, 1242–1251.
3. Robinson-Duggon, J., N. Mariño Ocampo, P. Barrías, D. Zuñiga-Núñez, G. Günther, A. Greer and D. Fuentealba (2019) Mechanism of visible-light photooxidative demethylation of toluidine blue O. *J. Phys. Chem. A*. **123**, 4863-4872.
4. Baptista, M. S., J. Cadet, P. Di Mascio, A. A. Ghogare, A. Greer, M. R. Hamblin, C. Lorente, S. C. Nunez, M. S. Ribeiro, A. H. Thomas, M. Vignoni and T. M. Yoshimura (2017) Type I and type II photosensitized oxidation reactions: guidelines and mechanistic pathways. *Photochem. Photobiol.* **93**, 912-919.
5. Baptista, M. S., J. Cadet, A. Greer and A. H. Thomas (2021) Photosensitization reactions of biomolecules: definition, targets, and mechanisms. *Photochem. Photobiol* **7** , 1456-1483.

6. Baptista, M. S., J. Cadet, A. Greer and A. H. Thomas (2023) Practical aspects in the study of biological photosensitization including reaction mechanisms and product analyses: A do's and don'ts guide. *Photochem. Photobiol*. **99**, 313-334.
7. Matikonda, S. S., D. A. Helmerich, M. Meub, G. Beliu, P. Kollmannsberger, A. Greer, M. Sauer and M. J. Schnermann (2021) Defining the basis of cyanine phototruncation enables a new approach to single molecule localization microscopy. *ACS Cent. Sci.* **7**, 1144-1155.
8. Butkevich, A. N., M. L. Bossi, G. V. Lukinavicius and S. W. Hell (2019) Triarylmethane fluorophores resistant to oxidative photobluing. *J. Am. Chem. Soc.* **141**, 981-989.
9. Gong, Q., X. Zhang, W. Li, X. Guo, Q. Wu, C. Yu, L. Jiao, Y. Xiao and E. Hao (2022) Long-wavelength photoconvertible dimeric BODIPYs for super-resolution single-molecule localization imaging in near-infrared emission. *J. Am. Chem. Soc.* **144**, 21992–21999.
10. Poljak, M., L. Wohlrabova, E. Palau, J. Nociarova, J. Misek, T. Slanina and P. Klán (2022) Chalcogen-based ratiometric reversible BODIPY redox sensors for the determination of enantioselective methionine sulfoxide reductase activity. *Chem. Commun.* **58,** 6389-6392.
11. Clennan, E. L. (2001) Persulfoxide: key intermediate in reactions of singlet oxygen with sulfides. *Acc. Chem. Res*. **34** ,875-884
12. Jiang, S., L. Carroll, L. M. Rasmussen and M. J. Davies (2021) Oxidation of protein disulfide bonds by singlet oxygen gives rise to glutathionylated proteins. *Redox Biol.* **38**, 101822.
13. Liu, F. and J. Liu, (2015) Oxidation dynamics of methionine with singlet oxygen: Effects of methionine ionization and microsolvation. *J. Phys. Chem. B*. **119**, 8001−8012.

14. E. L. Clennan; P. Dobrowolski and A. Greer (1995) Reaction of singlet oxygen with thietane. A novel example of a self-catalyzed reaction which provides evidence for a thiadioxirane intermediate. *J. Am. Chem. Soc.* **117**, 9800-9803.
15. Liang, J. J., C. L. Gu, M. L. Kacher and C. S. Foote (1983) Chemistry of singlet oxygen. 45. Mechanism of the photooxidation of sulfides. *J. Am. Chem. Soc* **105,** 4717–4721.
16. Bonesi, S. M., I. Manet, M. Freccero, M. Fagnoni and A. Albini (2006) Photosensitized oxidation of sulfides: Discriminating between the singlet oxygen mechanism and electron transfer involving superoxide anion or molecular oxygen. *Chem. Eur. J.* **12**, 4844-4857.
17. Bonesi, S. M., M. Fagnoni, S. Monti and A. Albini (2004) Photosensitized oxidation of phenyl and *tert*-butyl sulfides. *Photochem. Photobiol. Sci.* **3**, 489-493.
18. Yanke, C., M. Wanhong, R.Yanjun, C. Chuncheng, Z. Xinzhi, Z. Jincai and Z. Ling (2005) Photooxidation of dibenzothiophene and 4,6-dimethyldibenzothiophene sensitized by *N*-methylquinolinium tetrafluoborate: Mechanism and intermediates investigation. *J. Phys. Chem. B* **109**, 8270-8276.
19. Baciocchi, E., T. D. Giacco, F. Eliesi, M. F. Gerini, M. Guerra, A. Lapi and P. J. Liberali (2003) Electron transfer and singlet oxygen mechanisms in the photooxygenation of dibutyl sulfide and thioanisole in MeCN sensitized by *N*-methylquinolinium tetrafluoborate and 9,10-dicyanoanthracene. The probable involvement of a thiadioxirane intermediate in electron transfer photooxygenations. *J. Am. Chem. Soc.* **125**, 16444.
20. Manju, T., N. Manoj, J. L. Gejo, A. M. Braun and E. Oliveros (2014) Micellar control of the photooxidation pathways of 10-methyl phenothiazine: Electron versus energy transfer mechanisms. *Photochem. Photobiol. Sci.* **13**, 281-292.

21. Manju, T., N. Manoj, A. M. Braun and E. Oliveros (2012) Self sensitized photooxidation of *N*-methyl phenothiazine: Acidity control of the competition between electron and energy transfer mechanisms. *Photochem. Photobiol. Sci.* **11**, 1744-1755.

22. Zhang, D.,Y. Bin, L. Tallorin, F. Tse, B. Hernandez, E. V. Mathias, T. Stewart, R. Bau and M. Selke (2013) Sequential photooxidation of a Pt(II) (Diimine)cysteamine complex: intermolecular oxygen atom transfer versus sulfinate formation. *Inor. Chem*. **52**, 1676-1678.

23. Monsour, C. G., C. M. Decosto, B. J. Tafolla-Aguirre, L. A. Morales and M. Selke (2021) Singlet oxygen generation, quenching and reactivity with metal thiolate. *Photochem. Photobiol.* **97**, 1219-1240

24. Zhang, D., B. Hernandez and M. Selke (2008) Photooxidation of metal-bound thiolates: reactivity of sulfur containing peroxidic intermediates. *J. Sulfur Chem.* **29**, 377–388.

25. Hernandez, B., Y. Wang, D. Zhang and M. Selke (2006) Photooxidation of co-thiolato complexes in protic and aprotic solvents. *Chem. Comm.* 997–999.

26. Ohno, M., S. Kojima, Y. Shirakawa and S. Eguchi (1995) Hetero-diels-alder reaction of fullerene: Synthesis of thiochroman-fused C_{60} with *o*-thioquinone methide and oxidation to its *S*-oxides. *Tetrahedron Lett.* **36**, 6899–6902.

27. Mariño-Ocampo, N., J. S. Reyes, G. Günther, B. Heyne and D. Fuentealba (2022) Thiol-reacting toluidine blue derivatives: Synthesis, photophysical properties and covalent conjugation with human serum albumin. *Dyes Pigm*. **201**, 110225.

28. Robinson-Duggon, J., F. Pérez-Mora, L. Valverde-Vasquez, D. Cortés-Arriagada, J. R. De la Fuente, G. Günther and D. Fuentealba (2017) Supramolecular reversible on–off switch

for singlet oxygen using Cucurbit[n]uril inclusion complexes. *J. Phys. Chem. C.* **121**, 21782-21789.

29. Ogilby, P. R. and C. S. Foote (1983) Chemistry of singlet oxygen. 42. Effect of solvent, solvent isotopic substitution, and temperature on the lifetime of singlet molecular oxygen ($^1\Delta_g$). *J. Am. Chem. Soc.* **105**, 3423–3430.
30. Jensen, R. L., J. Arnbjerg and P. R. Ogilby (2010) Temperature effects on the solvent-dependent deactivation of singlet oxygen. *J. Am. Chem. Soc.* **132**, 8098-8105.
31. Aebisher, D., N. S. Azar, M. Zamadar, H. D. Gafney, N. Gandra, R. Gao and A. Greer (2008) Singlet oxygen chemistry in water. A porous Vycor glass-supported photosensitizer. *J. Phys. Chem. B* **112**, 1913-1917.
32. Butler, J., G. G. Jayson, A. J. Swallow (1975) The reaction between the superoxide anion radical and cytochrome c. *Biochim. Biophys. Acta Bioenerg.* **408**, 215-222.
33. Ortwerth, B. J., H. James, G. Simpson, M. Linetsky (1998) The generation of superoxide anions in glycation reactions with sugars, osones, and 3-deoxyosones. *Biochem. Biophys. Res. Comm.* **245**, 161-165.
34. Adam, W., W. Haas and B. B. Lohray (1991) Thianthrene 5-oxide as a mechanistic probe for assessing the electronic character of oxygen-transfer agents. *J. Am. Chem. Soc.* **113**, 6202-6208.
35. Bartholomew, R. F. and R. S. Davidson (1971) The photosensitised oxidation of amines. Part II. The use of dyes as photosensitisers: Evidence that singlet oxygen is not involved. *J. Chem. Soc. C*. 2347−2351.
36. Dantola, M. L., L. O. Reid, C. Castano, C. Lorente, E. Oliveros and A. H. Thomas (2017) Photosensitization of peptides and proteins by pterin derivatives. *Pteridines*. **28**, 105-114.

37. Alejandro, V., C. Layana, H. C. Junqueira, A. H. Thomas, R. Itri, M. S. Baptista and M. Vignoni (2021) Alkylation of a hydrophilic photosensitizer enhances the contact-dependent photo-induced oxidation of phospholipid membranes. *Dyes Pigm*. **187**, 109131.

38. Gu, C. L., C. S. Foote and M. L. Kacher (1981) Chemistry of singlet oxygen. 35. nature of intermediates in the photooxygenation of sulfides. *J. Am. Chem. Soc.* **103**, 5949-5951.

39. Foote, C. S. and J. W. Peters (1971) Chemistry of singlet oxygen. XIV. Reactive intermediate in sulfide photooxidation. *J. Am. Chem. Soc.* **93**, 3795–3796.

40. Jensen, F., A. Greer and E. L. Clennan (1998) Reaction of organic sulfides with singlet oxygen: A revised mechanism. *J. Am. Chem. Soc.* **120**, 4439-4449.

41. Clennan, E. L. and A. Greer (1996) The effect of alcohols on the photooxidative behavior of diethylsulfide. *J. Org. Chem.* **61**, 4793-4797.

42. Clennan, E. L. and K. Yang (1992) Remote Participation During Photooxidations at Sulfur. Evidence for Sulfurane Intermediates. *J. Org. Chem.* **57**, 4477-4487.

43. Clennan, E. L. and D. Aebisher (2002) The first example of a singlet oxygen induced double bond migration during sulfide photooxidation. Experimental evidence for sulfone formation via a hydroperoxy sulfonium ylide. *J. Org. Chem.* **67**, 1036-1037.

44. Toutchkine, A., E. L. Clennan (1999) The reactions of O_2 ($^1\Delta_g$) with anancomeric 1,3-dithianes. The first experimental evidence in support of a hydroperoxy sulfonium ylide as a precursor to sulfoxide on the sulfide singlet oxygen reaction surface. *J. Org. Chem*. **64**, 5620-5625.

45. Soni, D., N. Duvva, D. Badgurjar, T. K. Roy, S. Nimesh, G. Arya, L. Giribabu and R. Chitta (2018) Hypochlorite-mediated modulation of photoinduced electron transfer in a

phenothiazine-boron dipyrromethene electron donor-acceptor dyad: A highly water soluble "turn-on" fluorescent probe for hypochlorite. *Chem. Asian J.* **13**, 1594-1608.

46. Soni, D., S. Gangada, N. Duvva, T. K. Roy, S. Nimesh, G. Arya, L. Giribabu and R. Chitta (2017) Hypochlorite-promoted inhibition of photo-induced electron transfer in phenothiazine-borondipyrromethene donor-acceptor dyad: a cost-effective and metal-free "turn-on" fluorescent chemosensor for hypochlorite. *New J. Chem.* **41**, 5322-5333.
47. Petroff, J. T., K. N. Skubic, C. K. Arnatt and R. D. McCulla (2018) Asymmetric dibenzothiophene sulfones as fluorescent nuclear stains. *J. Org. Chem.* **83**, 14063-14068.
48. Frisch, M. J., G. W. Trucks, H. B. Schlegel, G. E. Scuseria, M. A. Robb, J. R. Cheeseman, G. Scalmani, V. Barone, G. A. Petersson, H. Nakatsuji, X. Li, M. Caricato, A. V. Marenich, J. Bloino, B. G. Janesko, R. Gomperts, B. Mennucci, H. P. Hratchian, J. V. Ortiz, A. F. Izmaylov, J. L. Sonnenberg, D. Williams-Young, F. Ding, F. Lipparini, F. Egidi, J. Goings, B. Peng, A. Petrone, T. Henderson, D. Ranasinghe, V. G. Zakrzewski, J. Gao, N. Rega, G. Zheng, W. Liang, M. Hada, M. Ehara, K. Toyota, R. Fukuda, J. Hasegawa, M. Ishida, T. Nakajima, Y. Honda, O. Kitao, H. Nakai, T. Vreven, K. Throssell, J. A. Montgomery, Jr., J. E. Peralta, F. Ogliaro, M. J. Bearpark, J. J. Heyd, E. N. Brothers, K. N. Kudin, V. N. Staroverov, T. A. Keith, R. Kobayashi, J. Normand, K. Raghavachari, A. P. Rendell, J. C. Burant, S. S. Iyengar, J. Tomasi, M. Cossi, J. M. Millam, M. Klene, C. Adamo, R. Cammi, J. W. Ochterski, R. L. Martin, K. Morokuma, O. Farkas, J. B. Foresman and D. J. Fox, *Gaussian 16*, Revision C.01; Gaussian, Inc.: Wallingford, CT, 2016.
49. Turque, O., R. M. O'Connor and A. Greer (2023) Singlet oxygen's potential role as a nonoxidative facilitator of disulfide S–S bond rotation. *Photochem. Photobiol.* **99***,* 652-660.

534

535